

## LONG-TERM CYCLIC TRIAXIAL TESTS WITH DEM SIMULATIONS

GIANLUCA ZORZI<sup>\*1</sup>, FABIAN KIRSCH<sup>1</sup>, FABIO GABRIELI<sup>2</sup> AND FRANK RACKWITZ<sup>3</sup>

<sup>1</sup> GuD Geotechnik und Dynamik Consult GmbH  
Darwinstraße 13, 10589, Berlin  
e-mail: zorzi@gudconsult.de, kirsch@gudconsult.de , web page: <http://www.gudconsult.de>

<sup>2</sup> Department of Civil Environmental and Architectural Engineering (ICEA)  
University of Padova  
Via Ognissanti 39, 35129 Padova, Italy  
e-mail: fabio.gabrieli@unipd.it, web page: <http://www.dicea.unipd.it>

<sup>3</sup> Soil Mechanics and Geotechnical Engineering Division,  
Technical University of Berlin  
Gustav-Meyer-Allee 25, 13355 Berlin, Germany  
e-mail: frank.rackwitz@tu-berlin.de,  
web page: [http://www.bau.tu-berlin.de/grundbau\\_und\\_bodenmechanik](http://www.bau.tu-berlin.de/grundbau_und_bodenmechanik)

**Key words:** DEM, cyclic loading, stress induced anisotropy

**Abstract.** Modeling the long-term performance of granular materials under cyclic loading conditions is still a challenge and a better understanding could provide a large benefit for the design of foundations. One typical application example are the foundations of wind turbines, for which the evolution of the soil mechanical behavior could lead to irreversible strain accumulation (with tilting and settlement) and dynamic resonance problems [1].

In this framework the Discrete Element Method [2] can provide useful information starting from a micromechanical point of view: it may allow engineers to increase their knowledge on the evolution of the mechanical behavior and to optimize the long-term design of these structures [3].

The present paper presents the capability of DEM to simulate a long-term cyclic drained triaxial test (up to 100,000 cycles). The results regard the progressive accumulation of plastic strain as function of the number of particles and the initial particles rearrangement. The influence of densification and contact orientation (anisotropy) in the evolution of the strength of the soil during the cyclic loading history is investigated.

### 1 INTRODUCTION

Repeated loadings are some of the main design driven factor for fatigue analysis of many civil structures like transportation facilities, industrial plant as well as wind turbine foundations. Considering the latter, which are subjected to millions of dynamic loadings during their lifetime, it is important to capture any change in soil properties which could have an impact on the behavior of the structure in terms of irreversible strain accumulation (settlement and tilting) and dynamic resonance problems [1].

Modeling accurately the evolution of soil properties under low amplitude cyclic stress loading is of great interest for geotechnical engineers, especially because there is a lack of accurate constitutive models focusing on these problems. During each loading cycle the soil experiences an accumulation of plastic deformations, with a partially open strain hysteresis loop. The smaller the loading amplitude is, the smaller the gap will be. These small vibrations and cyclic solicitations can be considered silent on the short term and the load-deformation behavior is quasi-elastic. However, in the long-term, they possibly result in a low but progressive degradation/damage of the structure and foundation, impacting the behavior of structures and their maintenance costs. Capturing this long-term behavior has been done applying different approaches in Finite Element Method (FEM). One is the application of the common engineering constitutive soil models (hysteretic approach), which is still a challenge and could possibly lead to inaccurate results due to the accumulation of numerical errors when hundred or thousand of cycles are applied [4]. Another strategy is to use the so-called explicit method such as the High Cycle Accumulation (HCA) model [4] or Cyclic Interaction Diagrams developed at NGI. The accumulation of plastic strains for a series of cyclic amplitude excitations are directly related to the number of cycles. These models are based on empirical macroscopic behavior of soil under cyclic loading obtained from experimental laboratory testing. However, the explicit models are either too much sophisticated or required extensive laboratory effort and are difficult to be used to analyze the soil behavior in other different loading conditions.

In the past decades Discrete Element Method (DEM, pioneered by Cundall et al. [2]) is becoming popular on simulating low amplitude cyclic triaxial tests, showing similarities to the overall macromechanical response of the laboratory tests and with the possibility to investigate the soil fabric evolution [6,7,8]. However, in those researches the application of rigid walls/membranes to simulate the real configuration required a large amount of particles and just few thousand of cycles were investigated. The DEM has proved to be a powerful method to study plasticity and non-linearity of granular materials which naturally arise from its intrinsic particle description without any particular mathematical hypothesis. Even though it is a good candidate for the comprehension and prediction of soil under cyclic loadings at a particles level point of view, its applicability in common geotechnical problems is still limited to the number of particles.

The present work shows the capability of DEM to simulate qualitatively a long-term cyclic drained triaxial test with low strain amplitude. The cyclic triaxial tests are simulated on a Representative Elementary Volume (REV) under stress-controlled conditions.

The trend of the accumulation of axial strains and strain amplitudes were analyzed in terms of reproducibility of the test results up to 10,000 cycles and with different number of particles (different REV sizes) up to 100,000 cycles. In the end, the analysis of the strength during different cyclic stages was linked to the evolution of the anisotropic soil fabric.

## **2 DISCRETE ELEMENT SIMULATIONS**

### **2.1 Sample Generation**

In the present analysis the DEM simulations were conducted using an open-source code YADE [9] based on a soft-particles approach. Spherical particles are considered to reduce the computational cost. The contact constitutive law is the classic elastic-plastic law with rolling

and twisting stiffness at the contact to take into account for grain roughness [9, 10]. The long-term cyclic drained triaxial tests are simulated with a cube-shaped cell called REV. A REV is characterized of Periodic Boundary (PB) conditions. Figure 1 is an example of a REV packing where the blank wire spheres are the exact copy from the opposite side.

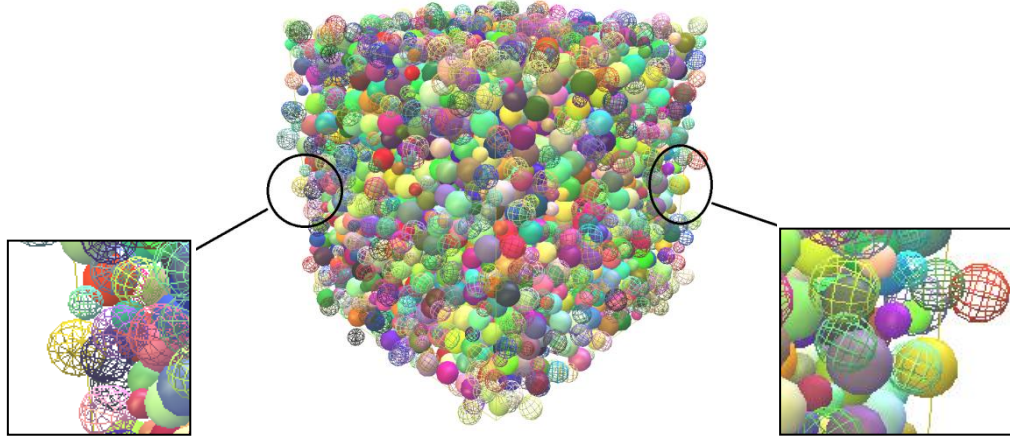


**Figure 1:** REV packing with periodic boundary conditions.

This configuration allows to use a smaller number of particles, which is important for computational reason and to avoid boundary effect problems arising when rigid-wall or membrane is used [11].

The aim of this paper is to show the capability of the DEM to simulate a long-term cyclic loading from a qualitative point of view and to study the initial departure of the grain assembly. Therefore, no contact law parameter calibration has been done but will be addressed in the future for a quantitative analysis of the cyclic behavior of soil. The contact parameters governing the macromechanical behavior are five and are listed in Table 1. These parameters represent an idealized cohesionless frictional material.

**Table 1:** Particles' contact parameters.

$E_c$ [Pa]	4e8
$\nu_c$ [-]	0.25
$\Phi_{ic}$ [°]	32
Beta [-]	0.75
Eta [-]	0.75
Density [kg/m <sup>3</sup> ]	2535

The samples were generated in order to match two predefined global quantities: Particles Size Distribution (PSD) and target porosity. A procedure for sample preparation similar to that described in [5] was adopted. A very loose cloud of particles with random position, high porosity (non-overlapping particles) and predefined PSD was generated in an initially large cube-shaped cell. An isotropic compression was applied with a high value of contact friction angle until a stable sample was achieved. At this stage the porosity of the sample is higher than the target one. A decrease in contact friction angle was gradually applied until the

desired porosity was reached. The sample preparation was considered finished when the unbalanced force [9], which is the ratio between inertia and interaction forces, went below  $10^{-3}$ . The contact friction angle was then set to the wanted value.

Regarding the PSD, the sample considered was a slightly uniform distribution with  $D_{\min}=4$  mm and  $D_{\max}=8$  mm. The target porosity for the sample preparation was set to be 0.50.

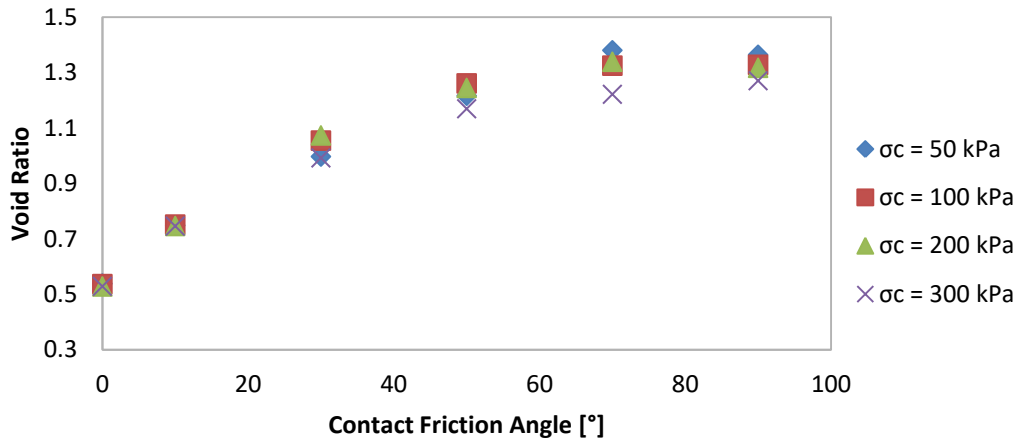


**Figure 2:** Void ratio of the REV for different friction angle and confining pressure.

The direct comparison in terms of porosity between laboratory and numerical samples, is not straightforward due to the difference in particles shape. Therefore, it would be more appropriate to compare relative densities and have different scales of minimum and maximum porosities between the laboratory and numerical samples. In order to have a complete overview of the relative state of density of the present sample, the minimum void ratio  $e_{\min}$  and maximum void ratio  $e_{\max}$  were calculated by imposing the contact friction angle to  $0^\circ$  and  $90^\circ$  respectively. The minimum and maximum void ratio depend on the confining pressure being used, thus different samples were generated with different contact friction angles and 4 different confining pressures. For all the confining pressures a low strain rate was set. It is important to underline that, during the sample preparation, the velocity of the boundaries under the isotropic confining pressure has to be as low as possible to avoid the creation of an inhomogeneous contact force distribution. As figure 2 shows, the denser state is characterized by a small variation of the minimum void ratio with different isotropic confining pressures while the loosest state is more scattered: this depends on the initial grain arrangement and chain force formation. The minimum and maximum void ratios at 100 kPa of confining pressure was adopted.  $e_{\min}$  and  $e_{\max}$  were equal to 0.537 and 1.32, respectively.

## 2.2 Triaxial Compression Test

Monotonic triaxial tests were conducted to analyze the macroscopic behavior of the sample. The lateral stress was kept constant at the confining pressure of 100kPa while the vertical boundaries were moved vertically under strain-control conditions. Two stable samples with 3000 particles and having different initial porosities were generated. The first, referred as "dense", has an initial porosity of 0.358 ( $I_D=0.97$ ). The second sample, named "loose", is characterized by an initial porosity of 0.50 ( $I_D=0.408$ ). The figures 3a and 3b

shows the deviatoric and volumetric behavior of the two samples.

The REV with 3,000 spheres mimics the classical drained triaxial compression test response of granular materials with different initial densities. Both samples reach the critical state with the same deviatoric shear stress and a quite constant volumetric strain. The loose state, which will be used for the cyclic loading triaxial test, shows the typical hardening behavior with shrinking.

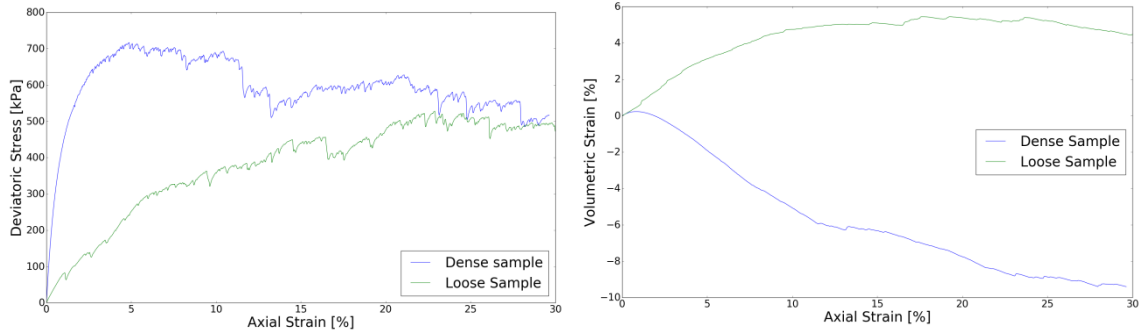


Figure 3: Triaxial test results of two DEM samples: (a) deviatoric and (b) volumetric behavior.

### 2.3 Cyclic Triaxial Test

Also in the simulation of the cyclic triaxial tests, the lateral confining pressure  $\sigma_c$  was kept constant at 100kPa while the vertical boundaries were cyclically moved under stress-control conditions. Figure 4 shows the cyclic stress path of the simulation in the  $p$ - $q$  plane, where  $p$  is the mean stress and  $q$  is the deviatoric stress. The first phase (horizontal red line) represents the isotropic confining phase up to a  $\sigma_c$  of 100kPa. Then the sample is sheared with a load  $\sigma_s$  of 40 kPa until the point  $(q_{av}, p_{av})$  is reached. The cyclic loading stage was then performed with a stress amplitude  $\sigma_{amp}$  of 30 kPa. The values of the loading stresses can be found in table 2.

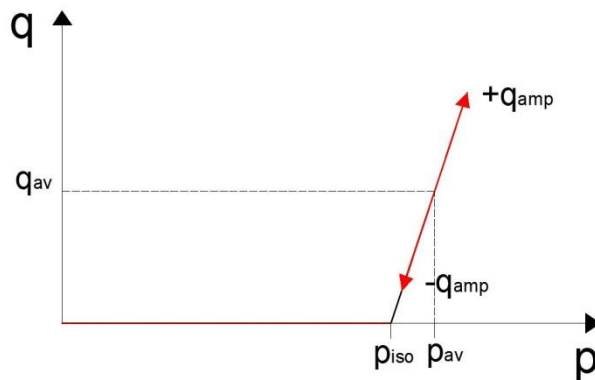


Figure 4: Cyclic Stress path

Table 2: Stress loading parameters

$p_{iso}$	100.00 kPa
$p_{av}$	113.33 kPa
$q_{av}$	40.00 kPa
$q_{amp}$	$\pm 30.00$ kPa

The mass of the PBs were adjusted in order to avoid inertial forces. The aim of the paper is to investigate the capability of the DEM to simulate the effect of a small strain amplitude on the long-term cyclic loading. Therefore, the cyclic stress was chosen in order to have a low cyclic strain amplitude of the order of  $10^{-3}$  and the static load far from failure. For small

number of particles in the REV and long-term cyclic loading, the chance of having an inhomogeneous distribution of contact forces is high (again the initial sample preparation has a strong influence on the behavior of the assembly). During the cyclic test, the occurrence of a chain buckling leads to a sudden large increase of plastic strain [6].

The analyses of the results of the DEM cyclic triaxial tests were done by following the procedure and the remarks explained in [12], which are depicted in figure 5 [12] for a laboratory cyclic triaxial test.

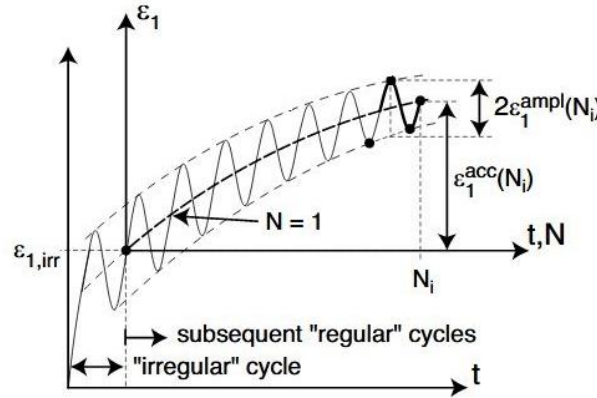


Figure 5: Cyclic Triaxial Test curve (modified from [12])

The cycles were divided in a first irregular cycle  $N_0$  in which there is the largest deformation and in subsequent regular cycles  $N_i$  ( $i=1, \dots, n$ ).

The trend of the axial strain during the cyclic triaxial test was analyzed by calculating the axial strain accumulation (1) and the axial strain amplitude (2) from the first regular cycle  $N_1$ [12].

$$\varepsilon_{1,i}^{acc} = \frac{1}{2} [\varepsilon_1^{max}(N_{i+1}) + \varepsilon_1^{min}(N_i)] \quad \text{where } i=1, \dots, n \text{ cycle} \quad (1)$$

$$\varepsilon_{1,i}^{amp} = \frac{1}{2} [\varepsilon_1^{max}(N_i) - \frac{1}{2} (\varepsilon_1^{min}(N_i) + \varepsilon_1^{min}(N_{i-1}))] \quad \text{where } i=1, \dots, n \text{ cycle} \quad (2)$$

The test was conducted using 3,000 spheres in a REV packing. The total number of cycles was 100,000. Figure 6 shows the trend of the axial strain accumulation plotted with the logarithm of the number of cycles. It is clearly visible that the rate of accumulation of axial strain decreases, reaching a constant value, which means that the soil reaches a stable configuration named shakedown state [13].

The shakedown state also emerges considering the trend of porosity as shown in figure 7. The first few thousand cycles are marked with the highest adaption period to the external cyclic solicitation, with the larger accumulation of permanent deformation. Subsequently to this adaption period, the material showed a resilient response to the increasing the number of cycle stresses, typical of the shakedown behavior [13].

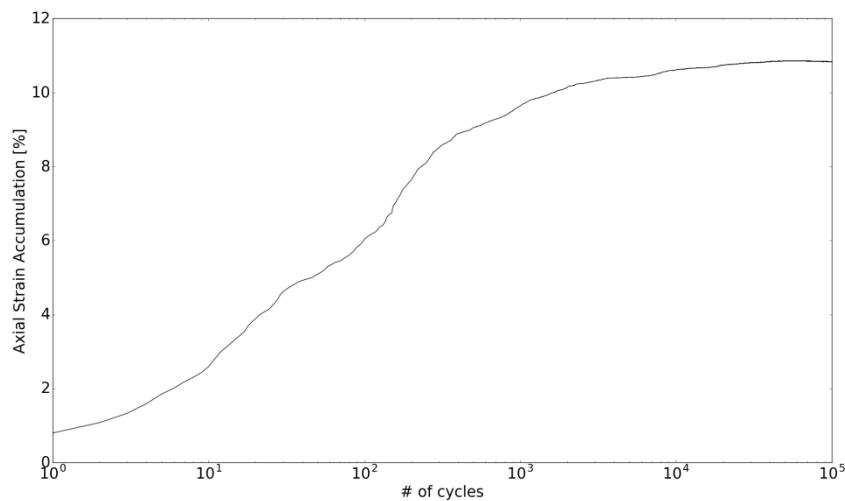


**Figure 6:** Axial Strain Accumulation of a REV with 3000 particles up to 100,000 cycles

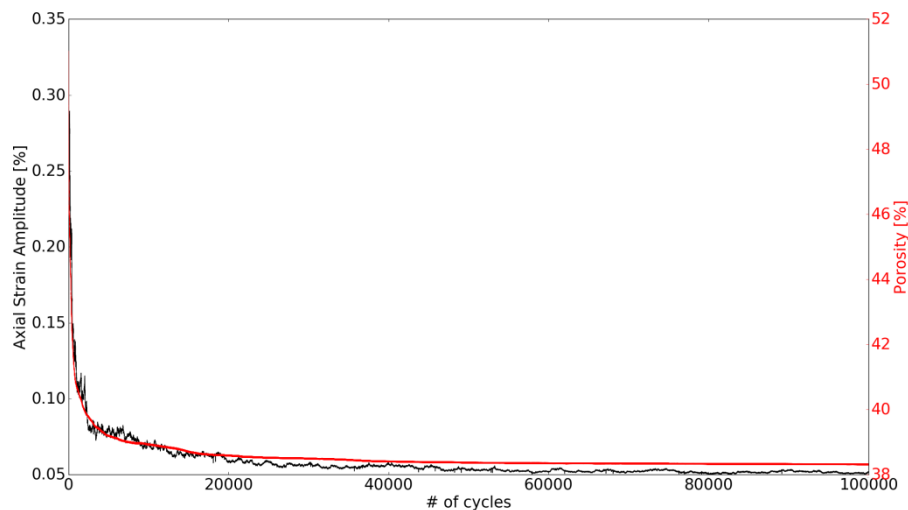


**Figure 7:** Trend of porosity (red line) and axial strain amplitude (black line) of a REV with 3000 particles up to 100,000 cycles

### 3. TEST REPEATABILITY OF CYCLIC TRIAXIAL TESTS

In the following, the degree of repeatability on the long-term cyclic behavior was investigated with different initial fabric and different number of particles. Different clouds of particles were prepared, with different initial random distributions and the procedure explained previously was used to create a stable packing.

Two different numbers of particles in a REV were considered: 2000 and 5000. For each number of particles, 10 samples were generated. The micromechanical parameters used in simulations are listed in table 1.

All the 20 samples were isotropically consolidated with a confining pressure of 100 kPa and cyclically loaded for 10,000 cycles. The target porosity during the sample preparation

was set 0.50 and from the inspection of the 20 samples the porosity differs of 0.03%.

Figure 8 shows the same cyclic behavior described earlier. The dispersion of the curves (i.e. repeatability) resulted lower with a large number of particles. This low variability is also depicted in figure 9, where the axial strain amplitude is plotted.

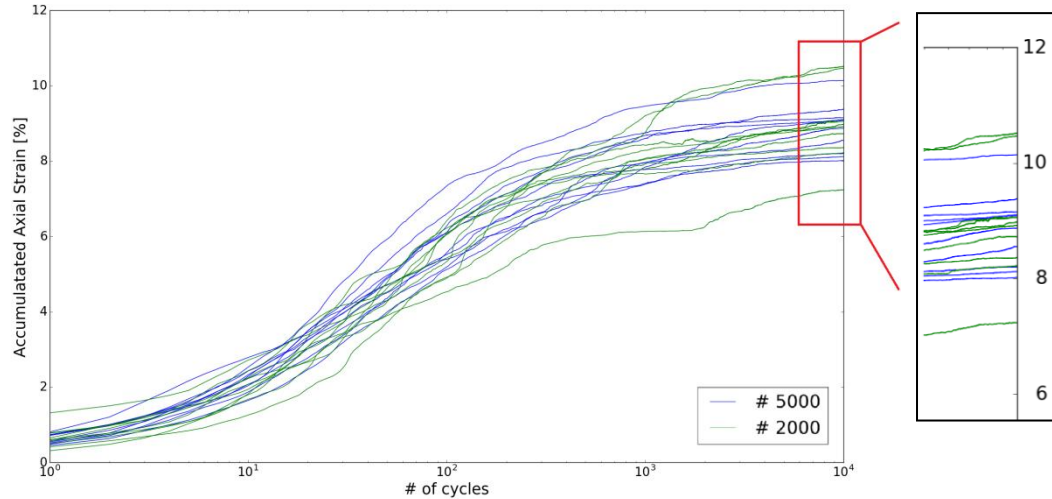


**Figure 8:** Axial Strain Accumulation for different initial packing.

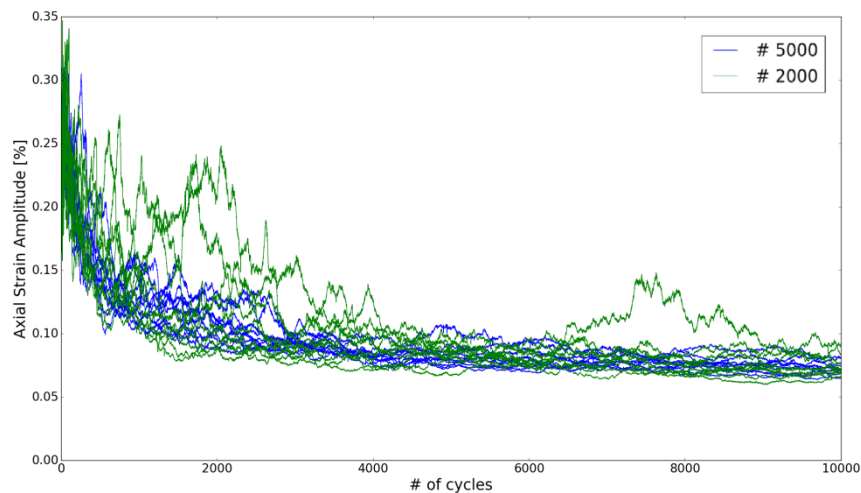


**Figure 9:** Axial Strain Amplitude for different initial packing.

#### 4 INFLUENCE OF THE REV SIZE ON THE LONG-TERM CYCLIC BEHAVIOR

With regards to the cyclic tests, the choice of the number of particles to be used in the REV is of capital importance from a computational stand point: the larger the number of particles is, the longer the simulation will be; on the other hand a too small number of particles may lead to incorrect or unreliable results.

A minimum number of particles should be used to get reliable porosity, coordination number, stress and strain values [14]. The evaluation of the minimum amount of spherical particles for a REV can be done by looking at the orientation distribution of the contact



normal which should be close to a sphere shape-like under isotropic compression[5].

Figure 10 shows the axial strain accumulation up to 100,000 cycles for different REV. The rapid increase of deformation for a small sample (with 500 particles) is due to buckling effect of large chain forces [6]. Moreover, specimens with a low number of particles can have a poor normal contact force distribution which governs the cyclic behavior. By increasing the number of particles per sample there is an increase of the axial strain accumulation.

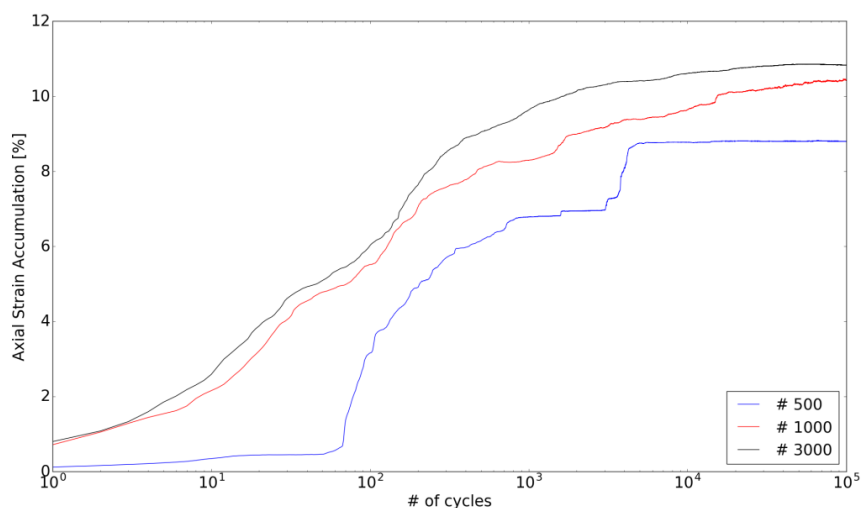


**Figure 10:** Axial Strain Accumulation as function of the # of particles for the sample.

## 5 STRENGTH AND STIFFNESS OF THE SAMPLE DURING CYCLIC STAGES

Cohesionless materials can benefit from low amplitude cyclic loading conditions, increasing their strength and stiffness after the cyclic loads. It is believed that this increment in stress is mainly due to the emergence of a densification process (decrease in porosity).

During the cyclic triaxial test for the REV with 3,000 spheres, the sample configuration was saved at 100/ 1,000/ 10,000/ 50,000/ 100,000 cycles, red points in figure 11. The samples were then unloaded until an isotropic confining pressure of 100kPa and the monotonic triaxial tests were conducted to analyze their strength and stiffness. The lateral stress was kept constant at the confining pressure of 100kPa while the vertical boundaries were moved vertically under strain-control conditions. In figure 12 and 13, it is clearly depicted that the sample is increasing its strength with the increasing of the number of cycles (solid lines), transforming from a typical hardening behavior with shirking (cycle 0) for loose material to a compaction-dilation behavior for dense materials.

At the same time, new samples were generated and monotonically sheared with the same exact porosity and isotropic confining pressure of 100kPa of the previously saved samples. Figure 12 and 13 show the difference between the monotonic triaxial tests of virgin samples (dashed lines) and cyclically loaded ones (solid lines) at the same porosity.

During a cyclic loading stress solicitation, the granular assembly decreases in density (behavior seen from a macroscopic point of view) but at the same time organizes its distribution of contact normal orientation in a favorable way to resist better against the external solicitation (stress induced anisotropy [6]). Figure 12 shows that the stress induced anisotropy (contact orientation) started to develop between 1,000 cycles (the red dashed and

solid lines are similar) and 10,000 cycles.

This effect could be studied with the DEM by analyzing the distribution of contact orientation. During the sample generation under an isotropic confining pressure and neglecting gravity, the contact orientation should reassemble a circular shape (isotropic fabric). After 100,000 cycles, the same distribution of contact orientation should evolve to adapt to the new stress conditions. Further investigation will be done to better characterized this phenomena.

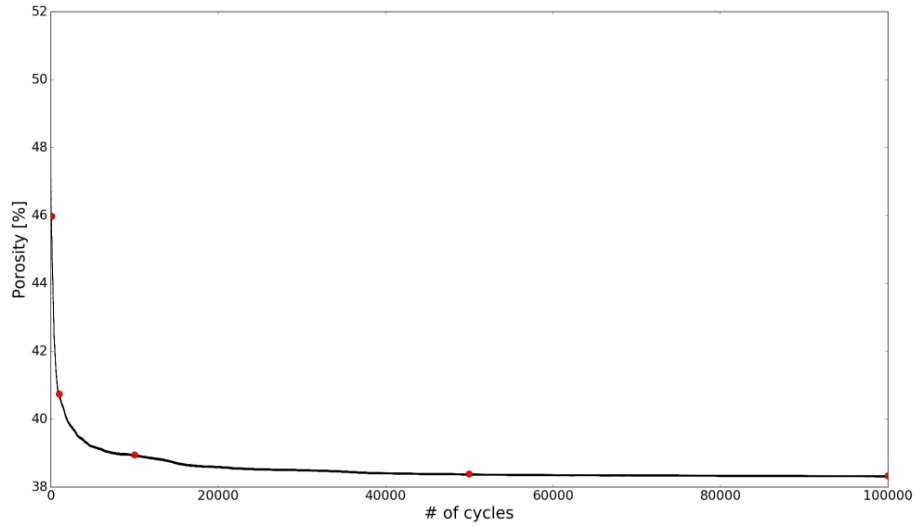


**Figure 11:** Porosity trend for 3,000 particles up to 100,000 cycles.

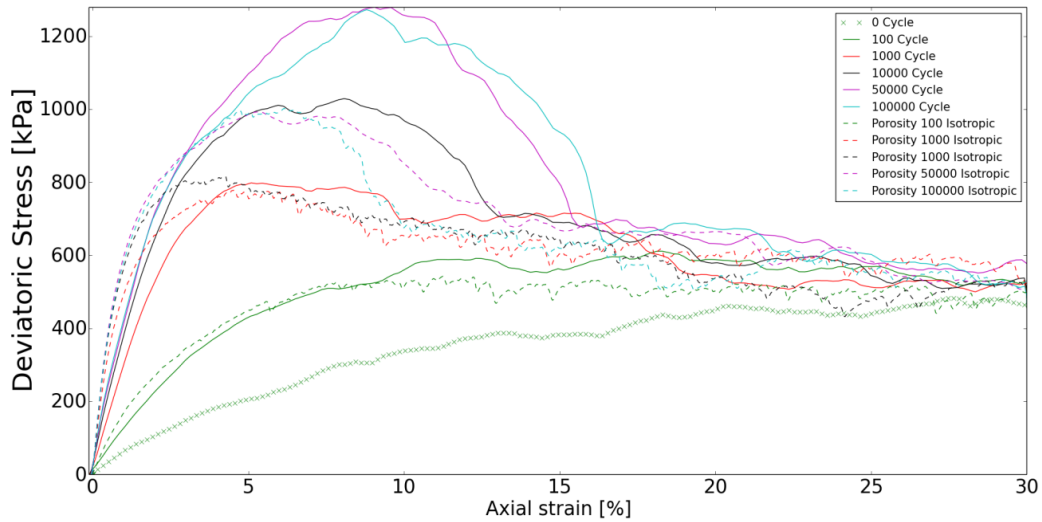


**Figure 12:** Triaxial tests results: deviatoric behavior. Solid line: anisotropic samples due to cyclic loading. Dashed line: isotropic samples.

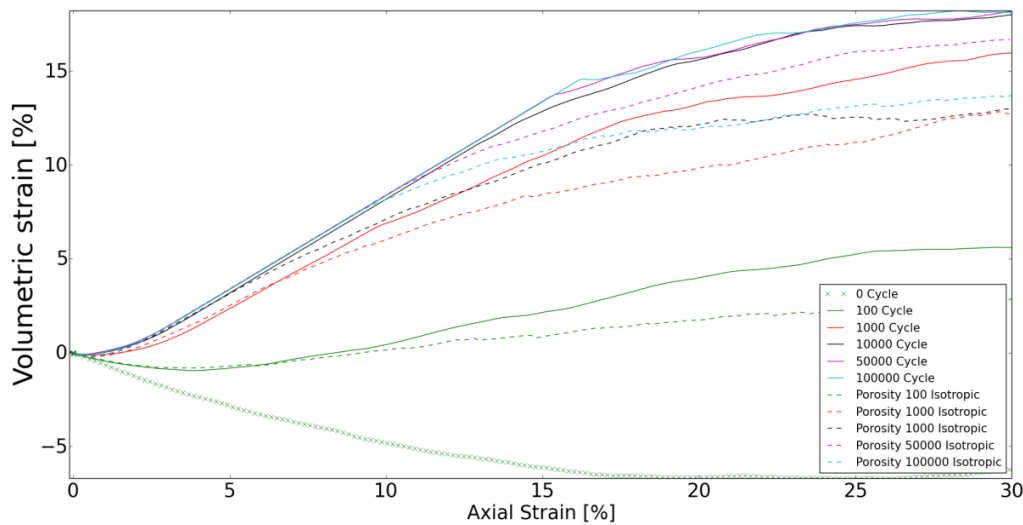


**Figure 13:** Triaxial tests results: volumetric behavior. Solid line: anisotropic samples due to cyclic loading. Dashed line: isotropic samples.

## 6 CONCLUSIONS

This paper shows the potentiality of DEM to simulate qualitatively a long-term cyclic triaxial test on a REV. The effect of different initial fabric and REV sizes have been investigated in relation to a large amount of cyclic loading. Future research will be to quantitative simulate cyclic triaxial test results of sand. It will allow a better understanding of the long-term behavior of granular materials from a micromechanical scale, possibly resulting as a base for an accurate formulation of constitutive models for cyclic loading.

## AKNOWLEDGEMENT



This research is part of the Innovation and Networking for Fatigue and Reliability Analysis of Structures - Training for Assessment of Risk (INFRASTAR) project.



This project has received funding from the European Union's Horizon 2020 research and innovation programme under the Marie Skłodowska-Curie grant agreement No 676139. The computing facilities offered by CloudVeneto (CSIA Padova and INFN) are acknowledged.

## REFERENCES

- [1] Bhattacharya, S. (2014). Challenges in Design of Foundations for Offshore Wind Turbines. Engineering & Technology Reference. <http://dx.doi.org/10.1049/etr.2014.0041>
- [2] Cundall, P. & Strack, O. (1979). A discrete numerical model for granular assemblies. *Géotechnique*, 29(1), 47-65. <http://dx.doi.org/10.1680/geot.1979.29.1.47>
- [3] O'Sullivan, C. & Cui, L. (2009). Fabric Evolution in Granular Materials Subject to Drained, Strain Controlled Cyclic Loading. *Powders And Grains 2009: Proceedings Of The 6Th International Conference On Micromechanics Of Granular Media*, 1145, 285-288. <http://dx.doi.org/10.1063/1.3179914>

- [4] Niemunis, A., Wichtmann, T., & Triantafyllidis, T. (2005). A high-cycle accumulation model for sand. *Computers And Geotechnics*, 32(4), 245-263. <http://dx.doi.org/10.1016/j.compgeo.2005.03.002>
- [5] Tong, A.-T., Catalano, E., Chareyre, B. (2012). Pore-scale flow simulations: model predictions compared with experiments on bi-dispersed granular assemblies, *Oil & Gas Science and Technology - Rev. IFP*, 67(35):743–752
- [6] Hu, M., O’Sullivan, C., Jardine, R., & Jiang, M. (2010). Stress-induced anisotropy in sand under cyclic loading. *Granular Matter*, 12(5), 469-476. <http://dx.doi.org/10.1007/s10035-010-0206-7>
- [7] Nguyen, N., François, S., & Degrande, G. (2014). Discrete modeling of strain accumulation in granular soils under low amplitude cyclic loading. *Computers And Geotechnics*, 62, 232-243. <http://dx.doi.org/10.1016/j.compgeo.2014.07.015>
- [8] O’Sullivan, C., Cui, L., & O’Neill, S. (2008). Discrete Element Analysis of the response of granular materials during cyclic loading. *Soils and Foundations*, 48(4), 511-530. <http://dx.doi.org/10.3208/sandf.48.511>
- [9] Šmilauer, V. et al. (2015), Yade Documentation 2nd ed. The Yade Project. DOI 10.5281/zenodo.34073
- [10] Widuliński, L., Kozicki, J., Tejchman, J. (2009). Numerical simulations of triaxial test with sand using DEM. *Archives of Hydroengineering and Environmental Mechanics*, 56 (3-4), 149-172.
- [11] Radjai, F., Dubois T. (2011). *Discrete-element modeling of granular materials*, Wiley-Iste, 181-198, 978-1-84821-260-2.
- [12] Wichtmann, T., Niemunis, A., & Triantafyllidis, T. (2009). On the determination of a set of material constants for a high-cycle accumulation model for non-cohesive soils. *International Journal For Numerical And Analytical Methods In Geomechanics*, n/a-n/a. <http://dx.doi.org/10.1002/nag.821>
- [13] García-Rojo, R., & Herrmann, H. (2005). Shakedown of unbound granular material. *Granular Matter*, 7(2-3), 109-118. <http://dx.doi.org/10.1007/s10035-004-0186-6>
- [14] Kawano, K, Sullivan, CO, Shire, T. (2016). Using DEM to assess the influence of stress and fabric inhomogeneity and anisotropy on susceptibility to suffusion. "Proc. 8th Int. Conf. Scour and Erosion, Harris, Whitehouse & Moxon (Eds.)", 85-94.